ARL 63-25

SUPERSONIC STAGNATION POINT HEAT TRANSFER TO HEMISPHERE CYLINDERS AT LOW REYNOLDS NUMBERS

H. TONG
W. H. GIEDT

UNIVERSITY OF CALIFORNIA
BERKELEY, CALIFORNIA

FEBRUARY 1963

AERONAUTICAL RESEARCH LABORATORIES
OFFICE OF AEROSPACE RESEARCH
UNITED STATES AIR FORCE

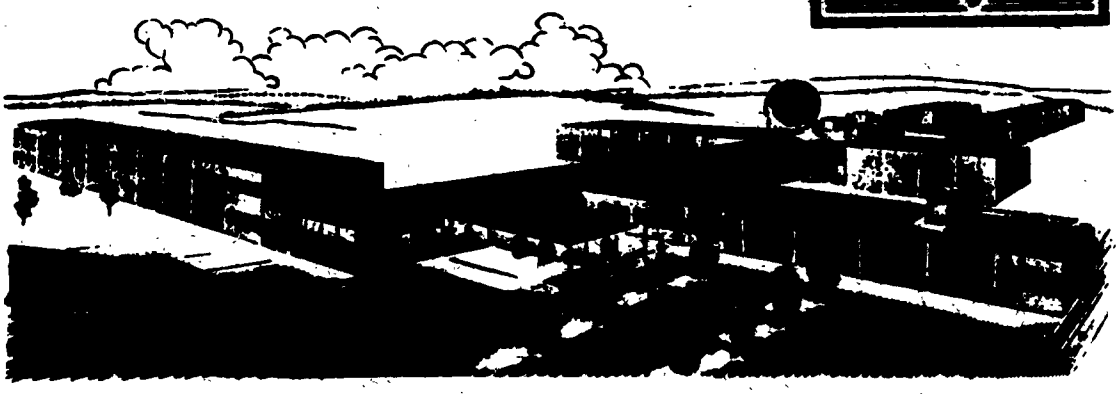

NOTICES

When Government drawings, specifications, or other data are used for any purpose other than in connection with a definitely related Government procurement operation, the United States Government thereby incurs no responsibility nor any obligation whatsoever; and the fact that the Government may have formulated, furnished, or in any way supplied the said drawings, specifications, or other data, is not to be regarded by implication or otherwise as in any manner licensing the holder or any other person or corporation, or conveying any rights or permission to manufacture, use, or sell any patented invention that may in any way be related thereto.

- - - - - - - - -

Qualified requesters may obtain copies of this report from the Armed Services Technical Information Agency, (ASTIA), Arlington Hall Station, Arlington 12, Virginia.

- - - - - - - - - -

This report has been released to the Office of Technical Services, U. S. Department of Commerce, Washington 25, D. C. for sale to the general public.

- - - - - - - - - -

Copies of ARL Technical Documentary Reports should not be returned to Aeronautical Research Laboratory unless return is required by security considerations, contractual obligations, or notices on a specific document.

AF-WP-L-APR 62 100

27-652, 300, 5-8-62

ARL 63-25

SUPERSONIC STAGNATION POINT HEAT TRANSFER TO HEMISPHERE CYLINDERS AT LOW REYNOLDS NUMBERS

H. TONG
W. H. GIEDT

UNIVERSITY OF CALIFORNIA
BERKELEY, CALIFORNIA

FEBRUARY 1963

CONTRACT AF 33(657)-8607
PROJECT 7064
TASK 7064-01

AERONAUTICAL RESEARCH LABORATORIES
OFFICE OF AEROSPACE RESEARCH
UNITED STATES AIR FORCE
WRIGHT-PATTERSON AIR FORCE BASE, OHIO

FOREWORD

This report was prepared at the Institute of Engineering Research, University of California, Berkeley, under Contract AF 33(657)-8607, Project 7064, "Aerothermodynamic Investigations in High Speed Flow," Task 7064-01, "Research on Hypersonic Flow Phenomena." The work was administered under the direction of the Aeronautical Research Laboratories, Office of Aerospace Research, USAF, with Capt. Walter W. Wells as Task Scientist.

The theoretical analysis and experimental work were carried out by H. Tong and W. H. Giedt under the supervision of Professors G. J. Maslach and S. A. Schaaf.

ABSTRACT

Stagnation point heat transfer at low Reynolds numbers in a supersonic air stream was investigated experimentally. A transient technique was employed using precooled thin-walled hemisphere-cylinder models. Tests were conducted at nominal Mach numbers of 2, 4, and 6, and in the Reynolds number range of 80 to 1500. Results are best represented by continuum boundary layer theory. Scatter was about ±10 per cent, so that any possible small shock wave-vorticity effect at the lower values of Reynolds number could not be identified.

TABLE OF CONTENTS

LIST OF ILLUSTRATIONS

NOMENCLATURE

c_p	specific heat at constant pressure
h	specific enthalpy
k	thermal conductivity
M	Mach number
Nu	Nusselt number
p	pressure
q	heat flux per unit area
Pr	Prandtl number
R	gas constant
r	radius
Re	Reynolds number $\frac{\rho U d}{\mu}$
T	absolute temperature, also $(T_o - T_w)$
U	velocity
x	distance from stagnation point
α, β	constants
δ	model wall thickness
γ	specific heat ratio
ϵ	density ratio across normal shock
λ	constant
μ	viscosity
ρ	density
τ	time

Subscripts

o	stagnation reservoir
1	upstream of shock
2	downstream of shock
BL	boundary layer value
e	edge of boundary layer
FM	free molecular flow value
s	stagnation behind shock
w	wall

I. INTRODUCTION

The flow field around a blunt body moving through the atmosphere at high velocities has not been adequately interpreted in the transition region between the continuum and free molecular flow regimes $(1 \gtrsim \frac{M_1}{R_1} \gtrsim 0.01)$. In regard to heat transfer and skin friction current opinion is that a modified boundary layer approach may be possible, if second order effects, ordinarily neglected in classical boundary layer, are considered. In particular, it has been pointed out that the vorticity introduced as the flow passes through the curved bow shock wave may increase the heat transfer and skin friction. Other second order effects which may enter are slip and temperature jump, boundary layer displacement of the flow, and body curvature.

Several studies of this transition region based on a modified boundary layer analysis have been reported. Of those in which heat transfer was considered two distinguishable approaches were followed. The first, used by Hayes and Probstein,[1] Hoshizaki,[2] Ho and Probstein,[3] and Cheng,[4] was based on treating the flow between the body and the bow shock as a single region. Hayes and Probstein and Hoshizaki assume the flow between the shock and the body to be incompressible. Similar results from a subsequent study by Ho and Probstein including compressibility would appear to justify this. Hoshizaki also included slip and temperature jump in his boundary conditions, but found their effects to be small.

Results are presented in terms of stagnation point heat transfer as a function of Reynolds number. To assess the importance of the second order effects, a comparison with continuum boundary layer theory (References 5 and 6) is also made. Hayes and Probstein, Hoshizaki, and Ho and Probstein

Manuscript released 18 December 1962 by the author for publication as an ARL Technical Documentary Report.

obtain similar results, which indicate an increase over continuum boundary layer (for values of $Re_2 \lesssim 1000$), which is dependent on the air stream velocity or density ratio across the shock (see Figures 1 and 2). Cheng, however, predicts an increase over the boundary layer theory starting at values of $Re_2 \cong 20{,}000$. In the range of $100 < Re_2 < 1000$ his results show approximately twice the increase as do those of Hayes and Probstein. Also of interest is the fact that after reaching a maximum his results decrease with decreasing Reynolds number toward free molecular flow theory.

The second approach was taken by Ferri, Zakkay and Ting[7] and by Van Dyke.[8] Their procedure was to define two regions between the shock and the body. The region near the body is assumed to be viscous, and that near the shock to be inviscid. Boundary conditions include specification of matching requirements at the interface. Both analyses predict an increase in heat transfer over continuum boundary layer theory. Van Dyke's results are comparable to those of Ho and Probstein. The increase predicted by Ferri, et.al., however, is from 200 to 300 percent higher, which is in general agreement with the results of Cheng. Stagnation point heat transfer data which agree with the latter theories have also been presented by Ferri, et.al.,[7,9]. This was obtained by using a transient technique in a blow-down type tunnel.

In view of the lack of agreement between the theories it was felt that additional experimental results were needed. The low density wind tunnel at the University of California can provide steady flow conditions in the upper part of the transition region. A program to obtain heat transfer data under steady state conditions was therefore

conducted. This is described in Reference 10. The results obtained are shown in Figure 1, where it will be seen that they agree best with the theories of Van Dyke and Hayes and Probstein. Also included are the recent and more applicable results of Van Dyke[11] for a free stream Mach number of 4 and a wall-to-stagnation temperature ratio of 0.5.

Although the experimental data available indicated substantially different trends, it was recognized that they were obtained in different test facilities and using different techniques. Because of this it was decided that some additional tests in the low pressure wind tunnel at the University of California using a transient technique would be desirable. This was therefore the objective of the present study. The basis of the technique is first reviewed. This is followed by a description of the models developed, the testing procedure and the results obtained.

II. THE TRANSIENT TECHNIQUE

In general, this method for determining heat rates is based on a knowledge of the temperature distributions with time in a suitably designed model. Evaluation of results may involve determination of both thermal capacity and conduction effects. For the present application it is convenient to utilize a thin-walled model. For convective heating to a thin-shell hemisphere the temperature distribution is governed by the following equation, where θ is measured from the stagnation point.[12]

$$q = \frac{k\delta}{r^2}\left[\frac{\cos\theta}{\sin\theta}\frac{\partial T}{\partial\theta} + \frac{\partial^2 T}{\partial\theta^2}\right] - \rho\,\delta\,c_p\,\frac{\partial T}{\partial\tau}$$

Here the first term represents the net conduction effect and the second term represents the rate of heat storage. Experimentally it is desirable to simplify the determination of the heat flux by evaluating q when the model wall is isothermal. Care must be exercised in assuring this condition, as it will be shown that small departures from the isothermal condition can introduce substantial effects.

To use the transient method the necessary initial temperature difference between model and free stream can be obtained by cooling or heating the model, raising the stagnation temperature above ambient temperature, or a combination of these methods. In this experiment stagnation temperature heating was not possible, so that the choice was between heating or cooling the model. The latter alternative was used since it was desirable to neglect the radiation heat exchange which for the same temperature difference would be greatest for heating.

Two procedures were considered for cooling the test models. The first was to fix the model in the test stream with a cooler that could be rapidly removed from the air stream, or alternatively, the model could be cooled and then rapidly moved into the air stream. Since advantages were not obvious, the latter alternative was used because of the simpler mechanism which could be employed.

In a transient heat transfer measurement radiation heat exchange and heat losses due to the thermocouple wires must be considered. The radiation heat exchange can be made negligible by using a polished model and small temperature differences. The effects of the thermocouple wire can be minimized by using model dimensions such that the effective thermal capacity of the model is large compared to that of the wire. This can be achieved by using large models and/or thick walls and small gauge thermocouple wire.

III. EXPERIMENTAL EQUIPMENT AND PROCEDURE

A. MODEL CONSTRUCTION

The models were formed by electroplating nickel onto an aluminum mandrel. The anode material was ordinary sheet nickel bent into the shape of a tube so that the mandrel was surrounded by the anode. The mandrel was mounted on a mechanism which imparted a reciprocating motion to it to achieve more uniform deposits. The electroplating bath was a standard Watts type (240 gm $NiSO_4$, 45 gms NiCl, and 30 gms Boric Acid per liter of water) maintained at a pH factor of 3 and a temperature of 50° C. The plating current was such that the deposition rate was approximately 0.001 inch per hour.

The models were easily removed from the mandrels by cooling the latter in cold water. They were then mounted on a jig and two 0.004 inch holes were drilled at the stagnation point for the thermocouple wires. 40 gauge copper-constantan wires were passed through individual holes and welded in place, using a capacity discharge welder. On the 0.5 inch in diameter model for which local temperature measurements were made at points other than the stagnation point, individual copper wires were welded at various locations on the model with the nickel model itself as the dissimilar metal. A second copper-constantan pair was welded at the base of this model. Thus it was possible to measure the temperature of the base and the temperature difference between the base and any desired location on the model.

No satisfactory data were available for the emf of copper-nickel junctions; hence it was necessary to calibrate the model junctions. This was accomplished by mounting the model on a liquid nitrogen cooled collar,

which was in turn mounted inside a ball jar. The jar was then evacuated to a pressure of about 40 microns of mercury to provide a controlled test condition. The stagnation point was heated by radiant energy from a nichrome coil to provide the necessary temperature difference on the model; thus a curve was obtained for the copper-nickel emf versus the copper-constantan emf.

The models were mounted on fiberglass-reinforced epoxy stings which had approximately the same coefficient of expansion as the nickel models, so that upon the cooling the model to sting joint would not be under excessive stress.

After completion of the tests the models were cast into an epoxy resin and cut in half along the axis. This surface was then polished to a fine finish and the local thickness of the model was measured on a toolmaker's microscope with a stage which had a least count of 0.0001 inch. Micro-photographs were also taken of the stagnation region using a metallograph. The wall thickness could thus be determined to an accuracy of 1 percent.

Three model sizes were used, 0.250 inch, 0.500 inch, and 1.000 inch diameter, with 0.004 inch nominal thicknesses. Two additional 0.250 inch diameter models were formed with wall thicknesses of approximately 0.007 and 0.011 inch to investigate the possible effects of heat losses due to the presence of the thermocouple wire.

A sectional drawing of a model is shown in Figure 3A, and the 0.500 inch and 0.250 inch diameter models as mounted in the wind tunnel are shown in Figures 4 and 5, respectively.

B. INSTRUMENTATION

The thermocouple emf was amplified with a Weston millivolt-microammeter and the variation of temperature with respect to time was recorded on a Minneapolis-Honeywell oscillograph. This arrangement provided a combination of high sensitivity and high recording speed. Sensitivities as high as 40 microvolts per inch were possible with negligible effects from extraneous noise signals. The response of the system was governed by the amplifier, which had a response time of approximately 0.1 second for a full scale step input.

The amplifier used is a balancing potentiometric instrument, and thus draws no current from the signal source. This simplified the calibration procedure in that a microvolt potentiometer could be used as the calibration signal with no correction for current flow. In cases where the amplifier was not used, the calibrations were performed by using an auxiliary voltage source in series with an equivalent thermocouple circuit resistance and measuring the magnitude of the source with a potentiometer.

C. EXPERIMENTAL PROCEDURE

All tests were conducted in the Number 4 Wind Tunnel at the University of California Aeronautical Sciences Laboratory. This tunnel is of the continuous flow type, operated by two five-stage steam ejectors with a maximum pumping capacity of about 70 pounds of air per hour. A complete description is given in Reference 13.

The test models were mounted on a high speed rotating octopus such that the model could be swung into the test section in about 0.3 second. An impact pressure probe was also mounted on the octopus such

nat when the model was out of the test section the probe was in the test section. In this way pressure measurements could be made while the model was being cooled.

Cooling of the models was accomplished by the flow of liquid nitrogen through a copper tube wound into a coil of approximately 1-1/4 inch inside diameter (Figure 5). One end of the coil was closed and the other end partially closed to accommodate the model to be cooled. The cooling coil was mounted on a traverse mechanism which permitted it to fully enclose the model. A spring-loaded trip device was used for the rapid removal of the cooling coil. When the coil was fully retracted, a mercury switch was activated, which started the rotation of the octopus and the recorder chart drive. To speed the cooling process a small quantity of nitrogen gas was bled into the closed end ot the coil. Thus between tests the model could be cooled in about 30 seconds. A typical experimental record is shown in Figure 6, where a chart speed of 5 inches per second was used.

IV. EVALUATION OF HEAT TRANSFER COEFFICIENTS

It is desirable to evaluate the heat transfer rates when the model is isothermal so that the conduction effects are zero. When this is true the temperature variation with time will be exponential; therefore the data were plotted on semi-log paper and the straight line portion was used to evaluate the heat transfer rate. To confirm that this corresponded to an isothermal wall condition, temperature distributions for the 0.500 inch diameter model were plotted. A typical plot is shown in Figure 6B. It was found that the isothermal time corresponded to about the middle of the exponential portion of the temperature-time plots.

At the time the model was isothermal the local heat rate could be determined from the equation

$$q = -\rho c_p \delta \frac{\partial T}{\partial \tau} \qquad (1)$$

where the model density was assumed constant at a value of 8.90 grams/cm^3, and its specific heat as a function of temperature was obtained from Reference 14, which is based on many published data. The local thickness was obtained from microphotographs of the model cross-section, as described earlier.

On the semi-log plots the straight line portion can be represented by

$$(T_o - T_w) = (T_o - T_w)_{\tau=0} \, e^{-\alpha\tau} \qquad (2)$$

where α is the slope of the line. Then

$$\frac{dT}{d\tau} = (T_o - T_w)_{\tau=0} \, \alpha \, e^{-\alpha\tau} \qquad (3) \quad .$$

and at $\tau = 0$

$$\left(\frac{dT}{d\tau}\right)_{\tau=0} = (T_o - T_w)_{\tau=0} \alpha \tag{4}$$

substituting into Equation (1) gives

$$q = -\rho \delta c_p (T_o - T_w)_{\tau=0} \alpha \tag{5}$$

Forming the Nusselt number

$$Nu = \frac{hd}{k} = \frac{d}{k} \frac{q}{(T_o - T_w)_{\tau=0}} \tag{6}$$

$$Nu = -\frac{d}{k} \rho \delta c_p \alpha \tag{7}$$

Stagnation point theory has shown that the velocity gradient at the edge of the boundary layer affects the heat transfer rate, and it is shown in the Appendix that this velocity gradient is dependent only on the Mach number; hence to account for the gradient the Nusselt number is divided by the square root of the non-dimensional velocity gradient

$$\sqrt{\tilde{u}_e'} = 1.681 \left[\frac{M_1^2 - 1}{1 + 0.2 M_1^2}\right]^{1/4} \tag{8}$$

which is obtained (see Appendix) for a value of $\gamma = 7/5$ and a pressure distribution given by

$$\frac{P_w - P_1}{P_{ws} - P_1} = \cos^2 \theta \ . \tag{9}$$

The Reynolds number is calculated for conditions behind the shock and is given by

$$Re_2 = \frac{\rho_2 U_2 d}{\mu_2} \tag{10}$$

which can be reduced for calculation to

$$Re_2 = 0.1685 \frac{p_2 M_2 d}{\mu_2 \sqrt{T_2}} \tag{11}$$

where p_2 is in inches of mercury

μ_2 is in $\frac{\text{lb-sec}}{\text{ft}^2}$ (evaluated at T_2)

T is in °R

d is in inches.

V. DISCUSSION

The necessary temperature difference between the test model wall and the stagnation temperature of the test air stream was obtained by cooling the model to approximately 130° K prior to exposing it to the supersonic jet. If the model were isothermal when first exposed to the jet, it would be sufficient to determine the gradient of temperature with respect to time directly from the temperature-time records by measuring the slope at the sudden rise in the record which represents exposure of the model to the jet. Because of the design of the cooling device, however, a small initial temperature gradient existed between the 90° point of the model and the stagnation point. The errors due to these small gradients have been estimated (see Appendix) and may be significant; it was therefore necessary to find a method of determining when the model was isothermal.

Inspection of the differential equation obtained from a heat balance on the hemispheric portion of the model shows that when the model is isothermal the temperature is an exponential function of time. Replotting the temperature-time behavior on a semi-log scale revealed that the temperature-time behavior was exponential for a short period of time, the length of this period increasing with increasing model size and decreasing heat rates. Reinspection of the differential equation indicated that although remote, it was possible for a temperature gradient to be such that the heat transferred by conduction could also be exponential. Thus it was not necessarily true that when the temperature was exponential with time, the model was isothermal.

To determine the temperature distribution when the temperature was exponential with time the 0.500 inch diameter model was instrumented

at positions other than the stagnation point. Typical distributions at several times are given in Figure 9, from which the time when the model was isothermal could easily be determined. This time corresponded very nearly to the middle of the exponential part of the stagnation point temperature-time curves.

Three 0.250 inch diameter models with nominal wall thicknesses of 0.004 inch, 0.007 inch, and 0.011 inch were used to check the effects of heat losses due to the thermocouple wires. It was found that the heat transfer rates calculated from the 0.004 inch wall model were approximately 12 percent less than those calculated from the 0.007 inch wall model and rates from the 0.007 and 0.011 inch wall models were in good agreement. A semi-empirical analysis was used to estimate the errors in the 0.500 and 1.000 inch diameter models (see Appendix). This analysis indicated that the errors would be small enough to warrant using the thin walls to achieve larger temperature-time gradients which could be more accurately measured.

On the basis of the experience gained in conducting this experiment it is felt that the minimum practical size for thin wall (0.004 inch) models for use in transient heat transfer measurements is about 0.500 inch diameter. 0.250 inch diameter models can be used if the wall thickness is approximately doubled, but only at low absolute heat transfer rates. It is also essential to know exactly when the models are isothermal if the calculation ignores the effect of conduction.

For future investigations it is recommended that consideration be given to locating the model in the stream and suddenly removing a cooling shield. It may be possible in this way to achieve a faster exposure of the

model to the airstream. Attention should be given in the design of the cooling shield so that it will make the model isothermal. Also in this regard it is noted that heating of air flowing through the tunnel would provide additional advantages. Higher initial temperature differences would be possible, and models could be cooled by allowing them to come to an isothermal condition at room temperature. Development of this latter suggestion should improve the accuracy with which the initial slope of the model temperature change can be determined.

VI. RESULTS AND CONCLUSIONS

The stagnation point heat transfer results determined as described in previous sections are listed in Table I. They are shown graphically in Figure 7 in terms of the Nusselt number divided by the square root of the dimensionless velocity gradient at the edge of the boundary layer, $Nu/\sqrt{\tilde{u}_e'}$, as a function of the Reynolds number downstream of the shock, Re_2. Generally several runs were made at each test condition. Evaluation of all the records thus obtained yielded duplicate results for most values of Re_2. Since the variation of $Nu/\sqrt{\tilde{u}_e'}$ obtained at any value of Re_2 was indicative of the experimental accuracy, all data points were included in Figure 7. As can be noted, only a few points fell outside the lines deviating ±10 per cent from the continuum boundary layer reference line.

An average $Nu/\sqrt{\tilde{u}_e'}$ was computed at each value of Re_2 for which two or more experimental points were available. The ratios of these average values to continuum boundary layer theory have been plotted as a function of Re_2 in Figure 8. The curve representing a least squares fit of the data reported in Reference 10 has also been included in this figure. Although the results from this investigation are in agreement with this curve, it should be noted that the data at the lower Reynolds numbers are primarily from the 0.250 inch model tested at $M_1 \sim 4.0$. In view of this and the experimental scatter, a firm conclusion regarding an increase over boundary layer theory is not considered justified.

The results are therefore considered to be in agreement with boundary layer theory over the range of Reynolds numbers investigated. However, since the trends predicted by the analyses of References 1, 2, 3, and 8 lie within the experimental scatter, it must be recognized that

small second order effects may be present. Reference to Figure 1 shows that the experimental results of Ferri, et.al.,[7,9] as well as the theory of Ferri[7] and Cheng[4] are significantly higher, and also show a deviation from continuum boundary layer theory at a much higher Reynolds number. It is noted that the data of Ferri, et.al., were obtained at higher stagnation temperatures (~ 2300 R compared to 530 R). This has been advanced as the reason for the differences in the theoretical predictions.[15] This explanation is, however, questioned by Van Dyke.[11]

In reviewing the findings of this investigation it is concluded that the transient technique developed for stagnation point heat transfer measurements yields results comparable in accuracy to the steady state technique used previously. Data obtained are in general agreement with the previous results[10] throughout the available Mach and Reynolds number ranges. In general, the data scatters about ±10 per cent above and below continuum boundary layer theory, but tend to cluster above at the lower values of Reynolds number. Although the predictions of References 1, 2, 3, and 8 are included in this scatter, no definite conclusion regarding second order effects can be reached.

REFERENCES

1. W. D. Hayes, R. F. Probstein — Hypersonic Flow Theory, Academic Press, New York, 1959.

2. H. Hoshizaki — "Shock Generated Vorticity at Low Reynolds Numbers," Lockheed Missiles & Space Division Report 48381, Vol. 1, pp. 9-43, 1959.

3. Hung Ta Ho, R. F. Probstein — "The Compressible Viscous Layer in Rarefied Hypersonic Flow," Rarefied Gas Dynamics, L. Talbot, ed., pp. 525-552, Academic Press, New York, 1961.

4. H. K. Cheng — "Hypersonic Shock-Layer Theory of the Stagnation Region at Low Reynolds Number," Proc. 1961 Heat Transfer & Fluid Mechanics Institute, June 1961, pp. 161-175.

5. M. J. Sibulkin — "Heat Transfer Near the Forward Stagnation Point of a Body of Revolution," J. Aero. Sci. 19, 8, 570, 1952.

6. J. A. Fay, F. R. Riddell — "Theory of Stagnation Point Heat Transfer in Dissociated Air," J. Aero. Sci., 25, 2, 73, 1958.

7. A. Ferri, V. Zakkay, L. Ting — "Blunt Body Heat Transfer at Hypersonic Speed and Low Reynolds Numbers," J. Aero. Sci. 28, 962, 1962.

8. M. Van Dyke — "Second-Order Compressible Boundary-Layer Theory with Application to Blunt Bodies in Hypersonic Flow," AFOSR-TN-61-1270, 1961.

9. A. Ferri, V. Zakkay — "Measurements of Stagnation Point Heat Transfer at Low Reynolds Numbers," ARL Tech. Report 38, 1961.

10. R. S. Hickman — "The Influence of Shock Wave-Boundary Layer Interaction on Heat Transfer to an Axisymmetric Body," Univ. of Calif. Eng. Proj. Report HE-150-191, 1962.

11. M. Van Dyke — "A Review and Extension of Second-Order Hypersonic Boundary-Layer Theory," Stanford Univ. Report SUDAER No. 127, 1962.

12. D. H. Crawford, W. D. McCauley — "Investigation of the Laminar Aerodynamic Heat Transfer Characteristics of a Hemisphere-Cylinder in the Langley 11-inch Hypersonic Tunnel at a Mach Number of 6.8," NACA Report 1323, 1957.

13. G. J. Maslach, F. S. Sherman — "Design and Testing of an Axisymmetric Hypersonic Nozzle for a Low Density Wind Tunnel," Univ. of Calif. Report WADC-TR-541, 1956. (Appendix D)

14. R. F. Hultgren — "Specific Heat Data Survey," Univ. of Calif. Dept. of Mineral Technology, Report YAC November 1960.

15. A. Ferri, V. Zakkay, L. Ting — "On Blunt-Body Heat Transfer at Hypersonic Speed and Low Reynolds Numbers," J. Aero/Space Sci. 29, 7, 382, 1962.

16. R. F. Probstein — "Continuum Theory and Rarefied Hyper Aerodynamics," in Rarefied Gas Dynamics, F. M. Devienne, ed., pp. 416-431, Pergamon Press, London, 1960.

17. R. F. Probstein, N. H. Kemp — "Viscous Aerodynamic Characteristics in Hypersonic Rarefied Gas Flow," J. Appl. Sci. 27, 3, 174, 1960.

18. J. Hilsenrath — "Tables of Thermal Properties of Gases," NBS Circular 564, 1956.

TABLE I. TABULATED RESULTS

1 inch Model

	M_1	Re_2	Nu	$Nu/\sqrt{u_e'}$ Run A	Run B	Run C	Run D	q/q_{BL}
	6.01	1485	62.0	25.6	27.1		26.7	0.993
	5.98	1260	56.2	23.2			24.7	0.980
○ 6	5.90	1071	51.0	18.6	23.2		22.0	0.944
	5.82	866	44.9	18.6		19.8		0.944
	5.64	640	44.0	18.3			16.6	1.080
	4.00	705	41.5	18.0				1.000
	3.98	614	39.1	16.9	17.3			1.017
~ 4	3.92	520	37.5	16.3	12.9	15.8		1.068
△	3.86	418	31.1	13.5	15.0		14.0	0.985
	3.70	314	27.0	11.9			13.5	1.001
	2.22	1019	44.5	22.3				1.002
	2.20	681	36.8	18.5				1.058
~ 2	2.18	549	31.8	16.1				1.028
□	2.18	549	32.9	16.7				1.065
	2.15	369	27.1	13.8				1.070

TABLE I - Continued.

1/2 inch Model

	M_1	Re_2	Nu	$Nu/\sqrt{\tilde{u}_e'}$				q/q_{BL}
				Run A	Run B	Run C	Run D	
	6.00	742	37.8	15.6				0.905
	5.92	586	37.0	15.3				0.945
~ 6	5.87	480	35.8	14.9				1.013
	5.78	394	30.7	12.8		12.1	13.1	0.962
	5.64	320	29.1	12.1	11.1			1.010
	4.01	349	28.9	12.5				1.000
	3.99	305	27.0	11.7	11.3			1.000
~ 4	3.90	232	25.7	11.2	9.9			1.096
	3.84	205	21.6	9.45				0.986
	3.71	156	20.0	8.78	8.0			1.049
	2.21	480	29.1	14.6				0.995
~ 2	2.20	275	23.5	11.8	12.5			1.061
	2.17	2.21	19.1	9.78	10.25			0.983
1/4 inch Model								
	~ 4.00	178			9.22		9.8	
	3.98	154	18.60	8.06	8.9		7.5	0.972
~ 4	3.93	131	17.80	7.75	8.08		7.65	1.011
	3.86	105	10.20	7.04	6.9		6.57	1.026
	3.73	77	14.43	6.33	5.62	5.51	6.40	1.079
		371			13.03			
		423			13.55			
~ 6		313			11.87			
		258		12.2	10.6			

APPENDIX

BOUNDARY LAYER HEAT TRANSFER RELATION

From Fay and Riddell[6] at the stagnation point

$$Nu_x = \frac{q\ Pr}{(h_o - h_{ws}) \left[\rho_{ws}\ \mu_{ws} \left(\frac{du_e}{dx} \right)_s \right]^{1/2}} \tag{A-1}$$

and

$$Nu_x = 0.67 \left(\frac{\rho_o\ \mu_o}{\rho_{ws}\ \mu_{ws}} \right)^{0.4} \tag{A-2}$$

where $Nu_x = \frac{q \times \bar{c}_p}{k(h_o - h_{ws})}$

and x is the local coordinate.

Equating Equations (A-1) and (A-2) gives

$$0.67 \left(\frac{\rho_o\ \mu_o}{\rho_{ws} \mu_{ws}} \right)^{0.4} = \frac{q\ Pr}{(h_o - h_{ws}) \left[\rho_{ws}\ \mu_{ws} \left(\frac{du_e}{dx} \right)_s \right]^{1/2}}$$

for low stagnation temperatures $\rho\mu \sim$ constant so that $(\rho_o \mu_o / \rho_w \mu_w) \sim 1$ and replacing $\rho_{ws}\mu_{ws}$ by $\rho_2 \mu_2$ we have

$$0.67 = \frac{q\ Pr}{(h_o - h_w) \left[\rho_2\ \mu_2 \left(\frac{du_e}{dx} \right)_s \right]^{1/2}} \tag{A-3}$$

for a perfect gas at the stagnation point

$$(h_o - h_{ws}) \sim c_p\ (T_o - T_{ws})$$

and since $Pr = \frac{\mu_2 c_{p2}}{k_2}$, Equation (A-3) can be written

$$0.67 = \frac{q\,d}{(T_s - T_w)\,k_2} \left[\frac{\mu_2 U_2}{U_2 \rho_2 d^2 \left(\frac{du_e}{dx}\right)_s} \right]^{1/2}$$

Defining the Nusselt and Reynolds numbers as

$$Nu \equiv \frac{h\,d}{k_2} = \frac{q\,d}{(T_o - T_{ws})\,k_2}$$

$$Re_2 \equiv \frac{\rho_2 U_2 d}{\mu_2} ,$$

we obtain

$$0.67 = \frac{Nu}{\sqrt{Re_2}} \frac{1}{\left[\frac{d}{U_2}\left(\frac{du_e}{dx}\right)_s\right]^{1/2}}$$

or

$$\frac{Nu}{\left[\frac{d\,(u_e/U_2)}{d\,(x/d)}\right]^{1/2}} = 0.67\sqrt{Re_2}$$

Defining $\frac{d\,(u_e/U_2)}{d\,(x/d)} \equiv \tilde{u}_e'$, the above expression becomes

$$\frac{Nu}{\sqrt{\tilde{u}_e'}} = 0.67\sqrt{Re_2} \qquad \text{(A-4)}$$

in which all properties and the velocity are based on conditions behind the normal part of the shock. Equation (A-4) is in agreement with the imcompressible theory of Sibulkin.[5]

DIMENSIONLESS VELOCITY GRADIENT

From Newton's Second Law

$$u_e \frac{du_e}{dx} = -\frac{1}{\rho_e} \frac{dp_e}{dx} \tag{B-1}$$

Differentiating once with respect to the x coordinate

$$u_e \frac{d^2u_e}{dx^2} + \left(\frac{du_e}{dx}\right)^2 = -\frac{1}{\rho_e} \frac{d^2p_e}{dx^2} + \frac{1}{\rho_e^2} \frac{dp_e}{dx} \frac{d\rho_e}{dx}$$

At the stagnation point $u_e = 0$ and $\rho_e \sim$ constant $= \rho_s$, and due to symmetry $(d\rho_e/dx) = 0$, so that

$$\left(\frac{du_e}{dx}\right)_s^2 = -\left(\frac{1}{\rho_s} \frac{d^2p_e}{dx^2}\right)_s . \tag{B-2}$$

For a hemisphere the pressure distribution is given by the modified Newtonian relation

$$\frac{p_e - p_1}{p_s - p_1} = \cos^2 \theta$$

since by the boundary layer concept $p_e \sim p_w$

Differentiating and noting that $x = r\theta$

$$\frac{dp_e}{dx} = -\frac{2}{r} (p_s - p_1) \cos \theta \sin \theta$$

$$\frac{d^2p_e}{dx^2} = -\frac{2}{r^2} (p_s - p_1) \left[\cos^2 \theta - \sin^2 \theta\right]$$

at the stagnation point

$$\cos \theta = 1 \quad \text{and} \quad \sin \theta = 0$$

so that

$$\left(\frac{d^2 p_e}{dx^2}\right)_s = -\frac{2}{r^2}(p_s - p_1)$$

substituting into (B-2) yields

$$\left(\frac{du_e}{dx}\right)^2_s = \frac{2}{\rho_s r^2}(p_s - p_1)$$

From the previous section

$$\tilde{u}_e' = \frac{d}{U_2}\left(\frac{du_e}{dx}\right)$$

then

$$\tilde{u}_e' = \frac{d}{U_2}\left[\frac{2}{\rho_s r^2}(p_s - p_1)\right]^{1/2}$$

$$= \frac{2}{U_2}\left[\frac{2}{\rho_s}(p_s - p_1)\right]^{1/2}$$

for a perfect gas $\frac{p}{\rho} = RT$

$$\tilde{u}_e' = \frac{2\sqrt{2}}{U_2}\left[RT_s - RT_s\frac{p_1}{p_s}\right]^{1/2}$$

$$= \frac{2\sqrt{2}}{U_2}\frac{\sqrt{\gamma RT_s}}{\sqrt{\gamma}}\left[1 - \frac{p_1}{p_s}\right]^{1/2}$$

$$= \frac{2\sqrt{2}}{M_2}\frac{1}{\sqrt{\gamma}}\left[1 - \frac{p_1}{p_s}\right]^{1/2}\sqrt{\frac{T_s}{T_2}} \qquad \text{(B-3)}$$

assuming $T_s \sim T_2$. Substituting the relations

$$\frac{p_1}{p_s} = \frac{\gamma+1}{2\gamma M_1^2 - (\gamma-1)}$$

and

$$M_2 = \left[\frac{M_1^2(\gamma-1) + 2}{2\gamma M_1^2 - (\gamma-1)} \right]^{1/2}$$

into Equation (B-3) leads to

$$\tilde{u}_e' = 2\sqrt{\frac{2}{\gamma}} \left[\frac{2\gamma M_1^2 - (\gamma-1)}{M_1^2(\gamma-1) + 2} \right]^{1/2} \left[1 - \frac{\gamma+1}{2\gamma M_1^2 - (\gamma-1)} \right]^{1/2}$$

$$= 2\sqrt{\frac{2}{\gamma}} \left[\frac{2\gamma M_1^2 - (\gamma-1)}{M_1^2(\gamma-1) + 2} \right]^{1/2} \left[\frac{2\gamma M_1^2 - (\gamma-1) - (\gamma+1)}{2\gamma M_1^2 - (\gamma-1)} \right]^{1/2}$$

$$= 2\sqrt{2} \left[\frac{M_1^2 - 1}{1 + \frac{\gamma-1}{2} M_1^2} \right]^{1/2}$$

Finally for $\gamma = 1.4$

$$\tilde{u}_e' = 2.88 \left[\frac{M_1^2 - 1}{1 + 0.2 M_1^2} \right]^{1/2} \qquad \text{(B-4)}$$

Probstein[16] defines the non-dimensional velocity gradient as

$$\frac{R}{U_1} \left(\frac{du_e}{dx} \right)_s = (1 - \epsilon) \sqrt{\frac{8}{3} \epsilon}$$

which can be written as

$$\tilde{u}_e' = \frac{d}{U_2} \left(\frac{du_e}{dx} \right)_s = 3.27 (1-\epsilon) \frac{M_1}{M_2} \sqrt{\frac{T_1 \rho_1}{T_2 \rho_2}} \qquad \text{(B-5)}$$

Probstein and Kemp[17] define the non-dimensional velocity gradient as

$$\frac{1}{U_1}\left(\frac{du_e}{dx}\right)_e = \sqrt{\frac{8}{3}\,\epsilon}$$

which can be written as

$$\tilde{u}_e' = 3.27\,\frac{M_1}{M_2}\,\sqrt{\frac{T_1\rho_1}{T_2\rho_2}} \qquad \text{(B-6)}$$

Relations (B-4), (B-5), and (B-6) are plotted in Figure 10 for comparison. Equation (B-4) was used in the calculations for this experiment.

ESTIMATE OF HEAT FLUX ERROR DUE TO SLOPE MEASUREMENTS

A simple fin solution for a hemisphere cap yields

$$q = + \frac{h\,\delta}{r^2}\left[\frac{\cos\theta}{\sin\theta}\,\frac{\partial T}{\partial\theta} + \frac{\partial^2 T}{\partial\theta^2}\right] - \rho\,\delta\,c_p\,\frac{\partial T}{\partial\tau}$$

where $T = (T_o - T_w)$. At the stagnation point this reduces to

$$q = + \frac{2\,k\,\delta}{r^2}\,\frac{\partial^2 T}{\partial\theta^2} - \rho\,\delta\,c_p\,\frac{\partial T}{\partial\tau} \qquad \text{(C-1)}$$

For the conditions

$$k \sim 0.7\ \frac{\text{watt}}{\text{cm}\ ^\circ\text{K}}\ , \quad \delta \sim 0.010\ \text{cm}\ , \quad \rho\delta = 0.089\ \frac{\text{gm}}{\text{cm}^2}\ ,$$

$$c_p \sim 0.3\ \text{Joules/gm}\ ^\circ\text{K}\ , \quad \text{and} \quad r^2 = 0.403\ \text{cm}^2\ \text{(0.5 inch model)},$$

$$q = + \frac{2 \times 0.7 \times 0.01}{0.403}\,\frac{\partial^2 T}{\partial\theta^2} - 0.089 \times 0.3\,\frac{\partial T}{\partial\tau}$$

$$= + 0.348\,\frac{\partial^2 T}{\partial\theta^2} - 0.0267\,\frac{\partial T}{\partial\tau} \qquad \text{(C-2)}$$

For the 0.500 inch model at $Re \sim 320$ and $M \sim 6$ the exponential portion of the temperature-time curve occurs at $\tau \approx 0.05$ sec. This has been verified to be the time when the model is isothermal. At $\tau = 0.10$ sec the temperature difference between the stagnation point and the 40° point is approximately 0.3 °K. If we assume a cosine temperature distribution

$$\frac{T_w - T_{90^\circ}}{T_{ws} - T_{90^\circ}} = \cos\theta \qquad \text{(C-3)}$$

$$T_{ws} - T_w = T_{ws} - T_{90°} - (T_{ws} - T_{90°}) \cos\theta$$

$$T_{ws} - T_w = (1 - \cos\theta)(T_{ws} - T_{90°}) \quad , \text{ and}$$

$$0.3 = (1 - 0.767)(T_{ws} - T_{90°})$$

$$T_{ws} - T_{90°} = 1.288$$

Therefore

$$\left(\frac{\partial^2 T}{\partial \theta^2}\right)_s = 1.288$$

and for the stated conditions $\frac{dT}{d\tau} \sim -27$ °K/sec.

Substituting into (C-2) gives

$$q = 1.288 \times 0.0348 + 0.0267 \times 27$$

$$= (0.045 + 0.721) \quad \text{watt/cm}^2$$

From this calculation we observe that the conduction term can be a large (4.8 percent in this case) portion of the total heat flux for relatively small temperature gradients along the model surface.

In the reduction of the data the temperature-time slopes were evaluated at the straight line portion of the semi-log plots and the large errors associated with small deviations from this time account for some of the scatter in the experimental results. It is estimated that the errors due to slope measurements are of the order of 5 - 6 percent.

ESTIMATE OF RADIATION HEAT EXCHANGE

Assuming that the test model is grey and the chamber a black isothermal enclosure, the radiation heat exchange can be expressed as

$$q = \epsilon_1 \sigma \left(T_1^4 - T_2^4\right) \qquad \sigma = 5.71 \times 10^{-12} \frac{\text{watts}}{\text{cm}^2\ ^\circ\text{K}}$$

where the subscripts 1 and 2 refer to the body and the enclosure, respectively. For polished nickel the emissivity for normal radiation is approximately 0.045 - 0.087 (see, for instance, Marks' Handbook) and for hemispheric radiation this value is increased about 20 percent so that an emissivity of 0.1 would form an upper bound on the heat exchanged by radiation. For ambient and wall temperatures of 300° K and 130° K, respectively

$$q = 0.10 \times 5.71 \times 10^{-12} \left(300^4 - 130^4\right)$$

$$\sim 0.0044 \quad \text{watts/cm}^2$$

The lowest heat rates measured were approximately 0.4 watts/cm^2, so that the maximum correction is of the order of 1 percent.

ERROR DUE TO PRESENCE OF THERMOCOUPLE WIRE

A heat balance on an element of a thermocouple wire yields

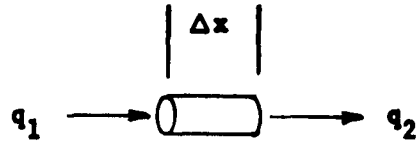

$$q_1 = -\left(A_x\, k \frac{\partial T}{\partial x}\right)_1 \qquad q_2 = -\left(A_x\, k \frac{\partial T}{\partial x}\right)_2$$

$$q_1 - q_2 = q_3 = \rho\, c_p\, A_x\, \Delta x \frac{\partial T}{\partial \tau}$$

Therefore

$$-\left(A_x\, k \frac{\partial T}{\partial x}\right)_1 - \left(-A_x\, k \frac{\partial T}{\partial x}\right)_2 = -\left(A_x\, k \frac{\partial^2 T}{\partial x^2}\right) \Delta x = \rho\, c_p\, A_x\, \Delta x \frac{\partial T}{\partial \tau}$$

or

$$\frac{\partial^2 T}{\partial x^2} = -\left(\frac{\rho\, c_p}{k}\right) \frac{\partial T}{\partial \tau} = -\beta^2 \frac{\partial T}{\partial \tau}$$

Assuming a solution of the form and letting

$$T = X(x)\, \Theta(\tau) \qquad = \qquad T_{aw} - T$$

gives

$$\frac{X''}{X} = -\beta^2 \frac{\Theta'}{\Theta} = \text{constant} = \lambda^2$$

Therefore,

$$\ln \Theta = -\frac{\lambda^2}{\beta^2}\, \Theta + \ln C_1$$

or

$$\Theta = C_1\, e^{-\frac{\lambda^2}{\beta^2}\, \tau}$$

and

$$X'' - \lambda^2 X = 0$$

The general solution of this equation is

$$X = C_2 e^{+\lambda x} + C_3 e^{-\lambda x}$$

Thus

$$T_{aw} - T = e^{-\frac{\lambda^2}{\beta^2}\tau} (C_2 e^{\lambda x} + C_3 e^{-\lambda x})$$

and $$\frac{\partial T}{\partial x} = e^{-\frac{\lambda^2}{\beta^2}\tau} \lambda (C_2 e^{\lambda x} - C_3 e^{-\lambda x})$$

Since

$$\frac{\partial T}{\partial x} \to 0 \quad \text{as} \quad x \to \infty, \quad C_2 = 0$$

Also

$$\frac{\partial T}{\partial \tau} = -\frac{\lambda^2}{\beta^2} C_3 e^{-\frac{\lambda^2}{\beta^2}\tau} e^{-\lambda x}$$

At $x = 0$ $\left(\frac{\partial T}{\partial x}\right)_{x=0} = -C_3 \lambda e^{-\frac{\lambda^2}{\beta^2}\tau}$

and

$$\left(\frac{\partial T}{\partial \tau}\right)_{x=0} = -C_3 \frac{\lambda^2}{\beta^2} e^{-\frac{\lambda^2}{2}\tau}$$

For the highest heat transfer conditions $\frac{\lambda^2}{\beta^2} \sim 0.25$ and $\left(\frac{\partial T}{\partial \tau}\right)_{\tau=0} \sim$ - 34.4 °K/sec, hence

$$C_3 \simeq 34.4 \frac{1}{0.25}$$

$$\sim 135$$

and $\left(\frac{\partial T}{\partial x}\right)_{\substack{x=0 \\ \tau=0}} \simeq 135\ ^\circ K/cm$.

Now for 0.003 inch wires

$$Q_1 = Q_{\substack{x=0 \\ \tau=0}} = -2\,k\,A_x \left(\frac{\partial T}{\partial x}\right)_{\substack{x=0 \\ \tau=0}}$$

$$= 2 \times 0.7 \frac{watt}{cm\ ^\circ K} \times 4.55 \times 10^{-5}\ cm^2 \times 135 \frac{^\circ K}{cm}$$

$$= 0.0086\ watt\ .$$

If we consider a disk with an area equivalent to an arc of the hemisphere, the heat flux stored in this element is

$$Q_2 = \rho\, c_p\, \delta\, A_s \frac{\partial T}{\partial \tau}$$

$$\sim \rho\, c_p\, \delta\, \pi\, (r \sin\theta)^2 \frac{\partial T}{\partial \tau}$$

and

$$Q = Q_1 + Q_2$$

The error is approximately $\frac{Q_1}{Q}$ and for the 1/4 inch model this was found to be ~ 12 percent. Estimating Q_2 from the measured value of $\partial T/\partial \tau$ gives

$$Q_2 = 8.9 \times 0.3 \times 0.01 \times 3.14 \times 0.101 \sin^2\theta \times 34.4$$

$$= 0.292 \sin^2\theta$$

The value of θ is now determined by noting

$$\frac{Q_1}{Q_1 + Q_2} = 0.12$$

and

$$Q_1 = 0.12\ (Q_1 + Q_2)$$

$$Q_2 = \frac{Q_1}{0.12} - Q_1 = 7.34\ Q_1$$

Therefore

$$0.292 \sin^2 \theta = 7.34 \times 0.0086$$

$$\sin^2 \theta = 0.216$$

$$\sin \theta = 0.465$$

$$\theta = 26.8°$$

Assuming that the same surface area is involved (and wall to wire thickness which was held constant), for the 1/2 inch model for the same conditions

$$Q_2 \sim 0.544 \text{ watt}$$

and

$$\frac{Q_1}{Q} = \frac{0.0086}{0.0086 + 0.544} = 1.7\% \ .$$

Similarly for the 1 inch model the error is found to be ~ 0.4 percent.

From this approximate calculation we conclude that the results as presented may be systematically low by 1.7 and 0.4 percent for the 1/2 inch and 1 inch diameter models, respectively.

ERROR ANALYSIS FOR INSTRUMENTATION

The heat transfer coefficient is

$$Nu = -\frac{d}{k} \rho \delta c_p \alpha$$

The errors due to the quantity $d\rho\ \delta$ are systematic and the values of c_p and k are obtained from published data[18] and assumed accurate. The remaining quantity is α so that the maximum probable error in this value is the maximum probable error in the Nusselt number. From Section IV we have

$$\left(\frac{dT}{d\tau}\right)_{\tau=0} = (T_o - T_{\tau=0})\ \alpha$$

$$\alpha = \frac{\left(\frac{dT}{d\tau}\right)_{\tau=0}}{(T_o - T_{\tau=0})}$$

The probable error can be written as

$$\frac{E_\alpha}{\alpha} = \left[\left[\frac{E_{(dT/d\tau)}}{dt/d\tau} \right]^2 + \left[\frac{E_{(T-T_{\tau=0})}}{(T-T_{\tau=0})} \right]^2 \right]^{1/2}$$

The errors in the slope measurements have already been estimated to be ~ 6 percent. The error in the temperature measurements depends on the calibration source and the ability to read the records. This error is probably less than 3 percent. Hence

$$\frac{E_\alpha}{\alpha} = [0.0036 + 0.0009]^{1/2}$$

$$= 6.7\% .$$

From Section IV the Reynolds number is

$$Re_2 = 0.1685 \frac{p_2 M_2 d}{\mu_2 \sqrt{T_2}}$$

The errors in M_2 are negligible since behind the shock the Mach number is a very small function of the pressure ratio p_{2s}/p_o. The error in d will be systematic, so that

$$Re_2 = K \frac{p_2}{\mu_2 \sqrt{T_2}}$$

where K is a constant. Assuming a linear viscosity law $\mu_2 \sim T_2$ and noting that at a given Mach number $T_2 \sim T_o$ we have

$$Re_2 = K \frac{p_2}{(T_o)^{3/2}}$$

The probable error can be written as

$$\frac{E_{Re_2}}{Re} = \left[\left[\frac{E_{p_2}}{p_2} \right]^2 + \left[\frac{3}{2} \frac{E_{T_2}}{T_2} \right]^2 \right]^{1/2}$$

All impact pressures were measured with an oil manometer with a least count of 0.001 inch. Stream variations with time are about twice this magnitude. The lowest impact pressures measured were ~ 0.500 inch, so that the error due to this source would be 0.4 percent. Stagnation temperature measurements could be read to within 1.0°F, and for an ambient temperature of 540°R the error is ~ 0.2 percent. Hence

$$\frac{E_{Re}}{Re} = [8 \times 10^{-6}\ 4.50 + 10^{-6}]^{1/2}$$

$$= 0.5\% .$$

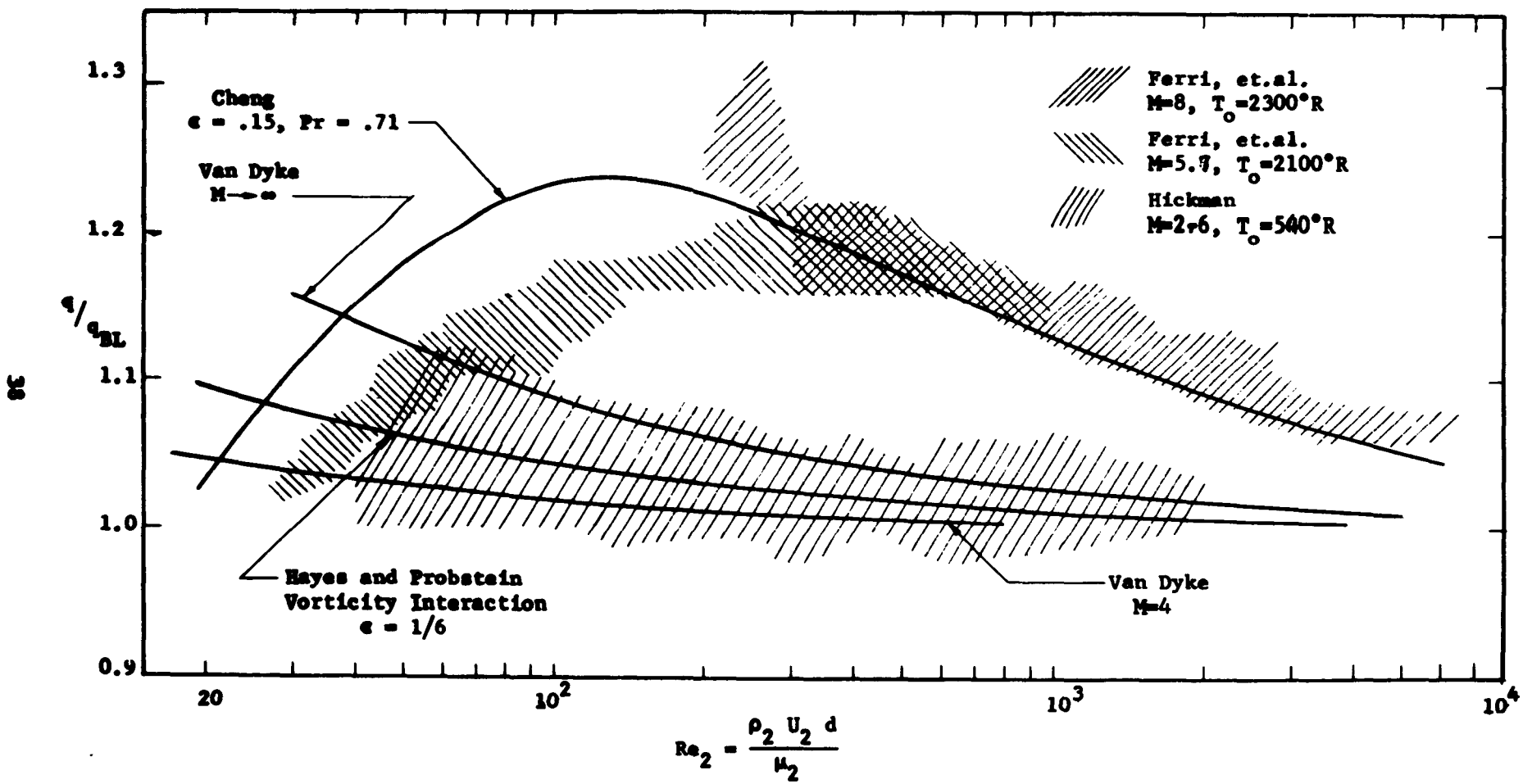

FIGURE 1. COMPARISON OF THEORETICAL AND EXPERIMENTAL STAGNATION POINT HEAT TRANSFER

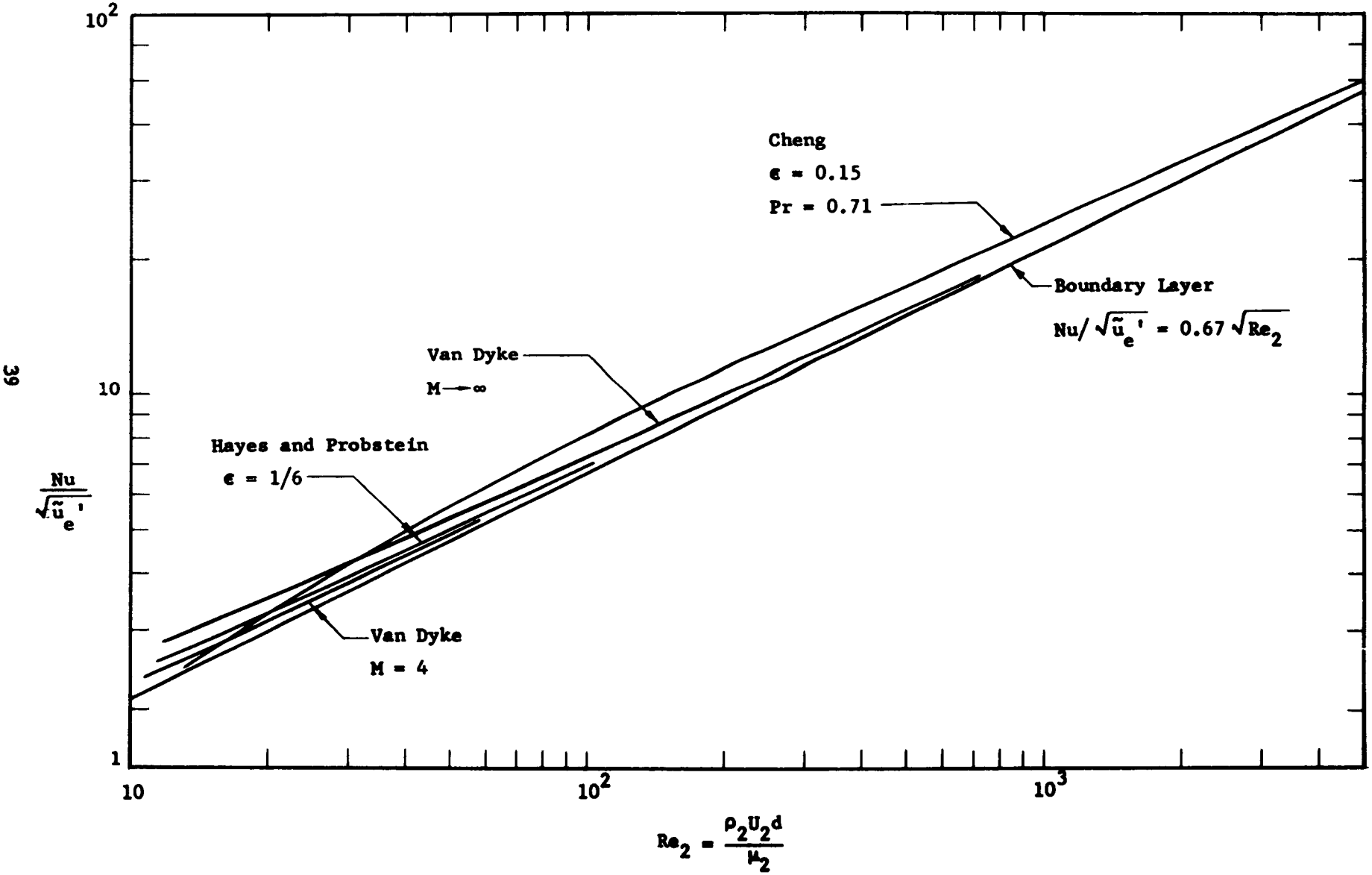

FIGURE 2. COMPARISON OF THEORETICAL STAGNATION POINT HEAT TRANSFER AT LOW REYNOLDS NUMBERS

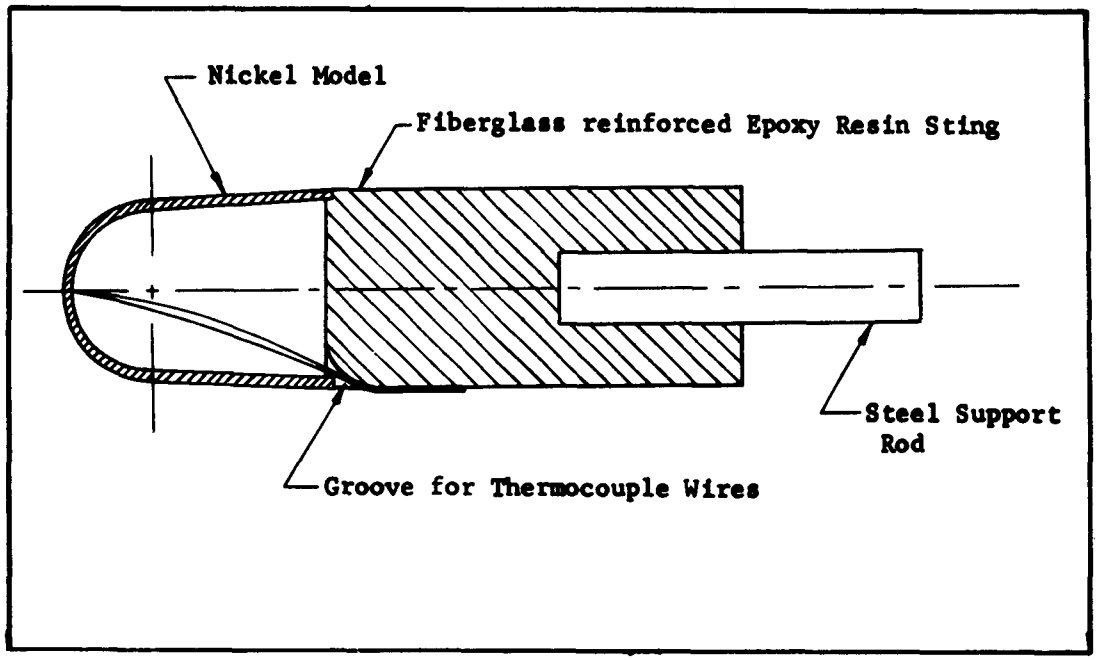

Figure 3A. SECTIONAL DRAWING OF HEAT TRANSFER MODEL

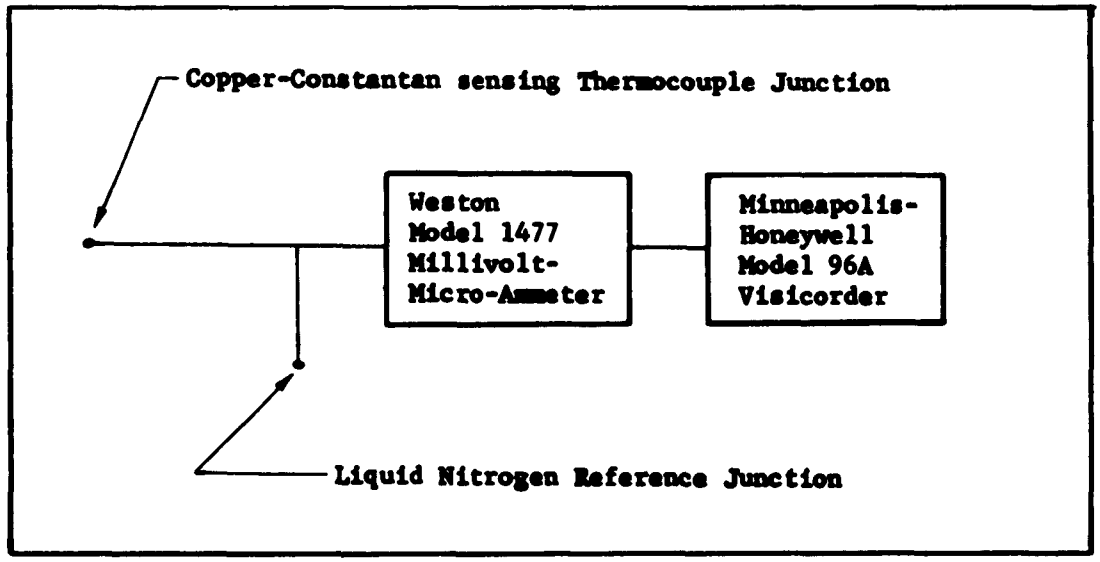

Figure 3B. Instrumentation Block Diagram

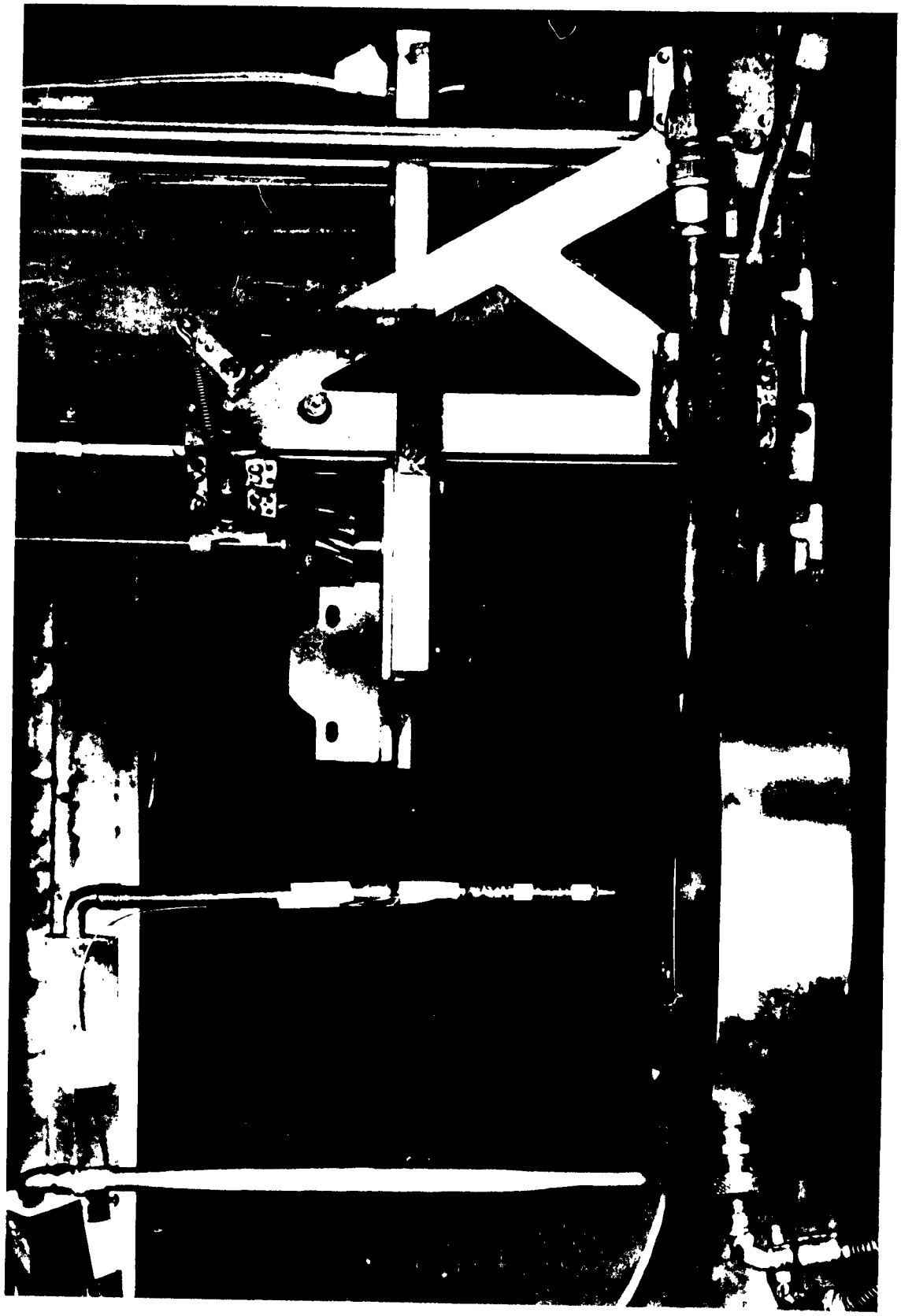

FIGURE 4. 0.250 INCH DIAMETER HEAT TRANSFER MODEL IN TEST POSITION

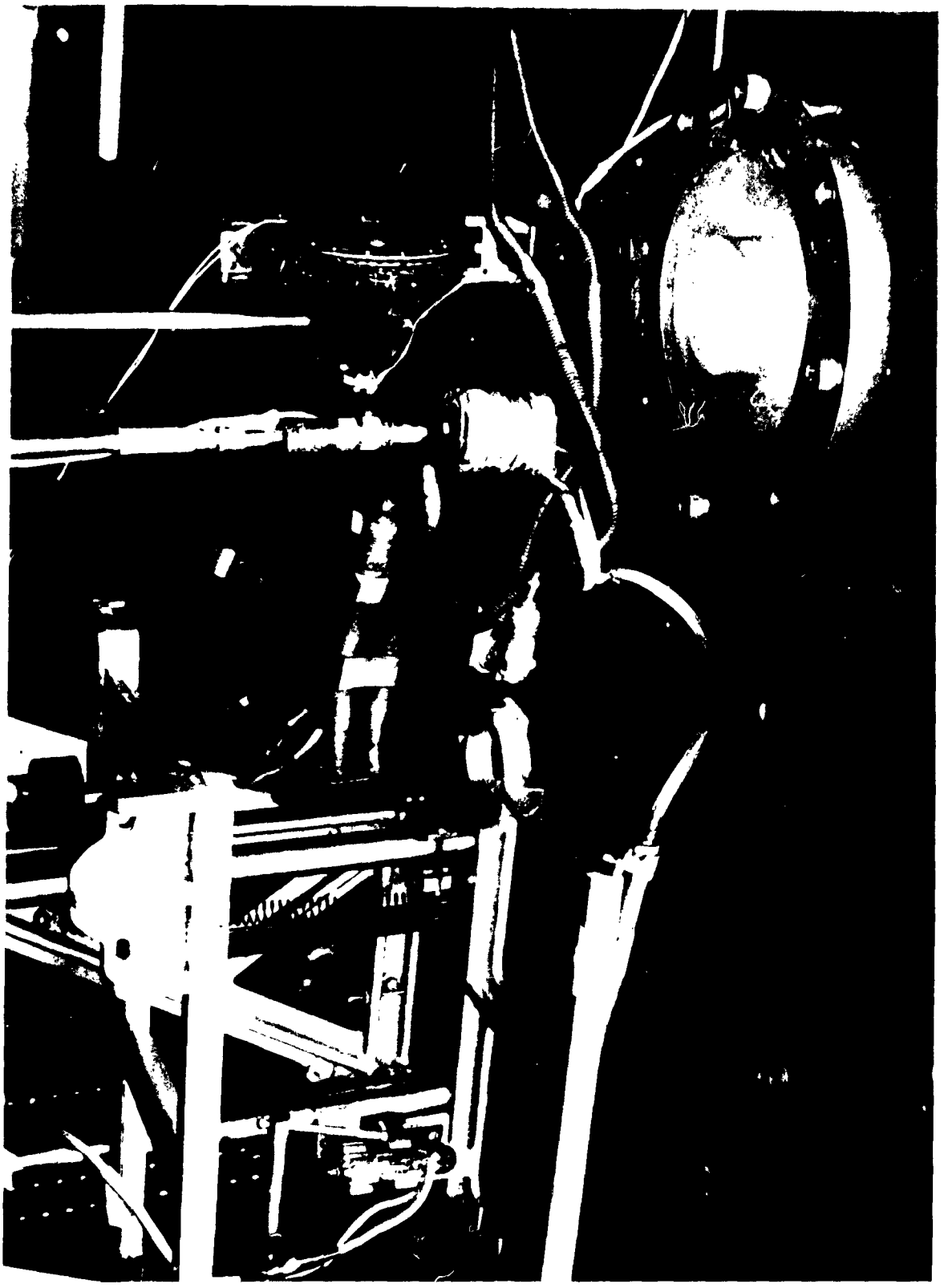

FIGURE 5. 0.500 INCH DIAMETER MODEL BEFORE COOLING

Typical Temperature Time Record

Figure 6A

Typical Semi-Log Temperature-Time Plot

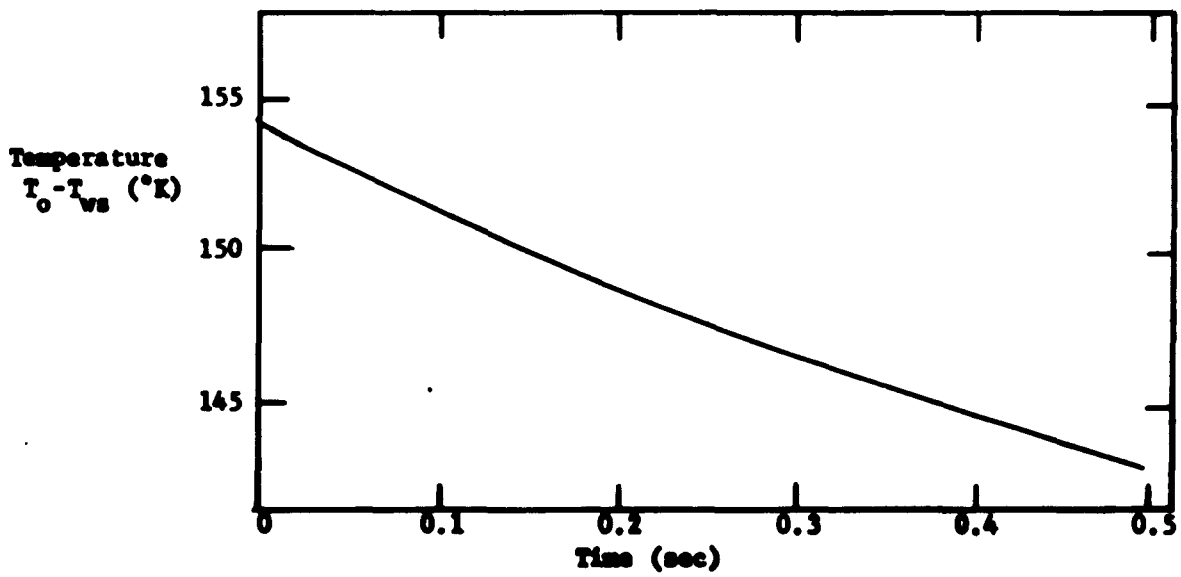

Figure 6B

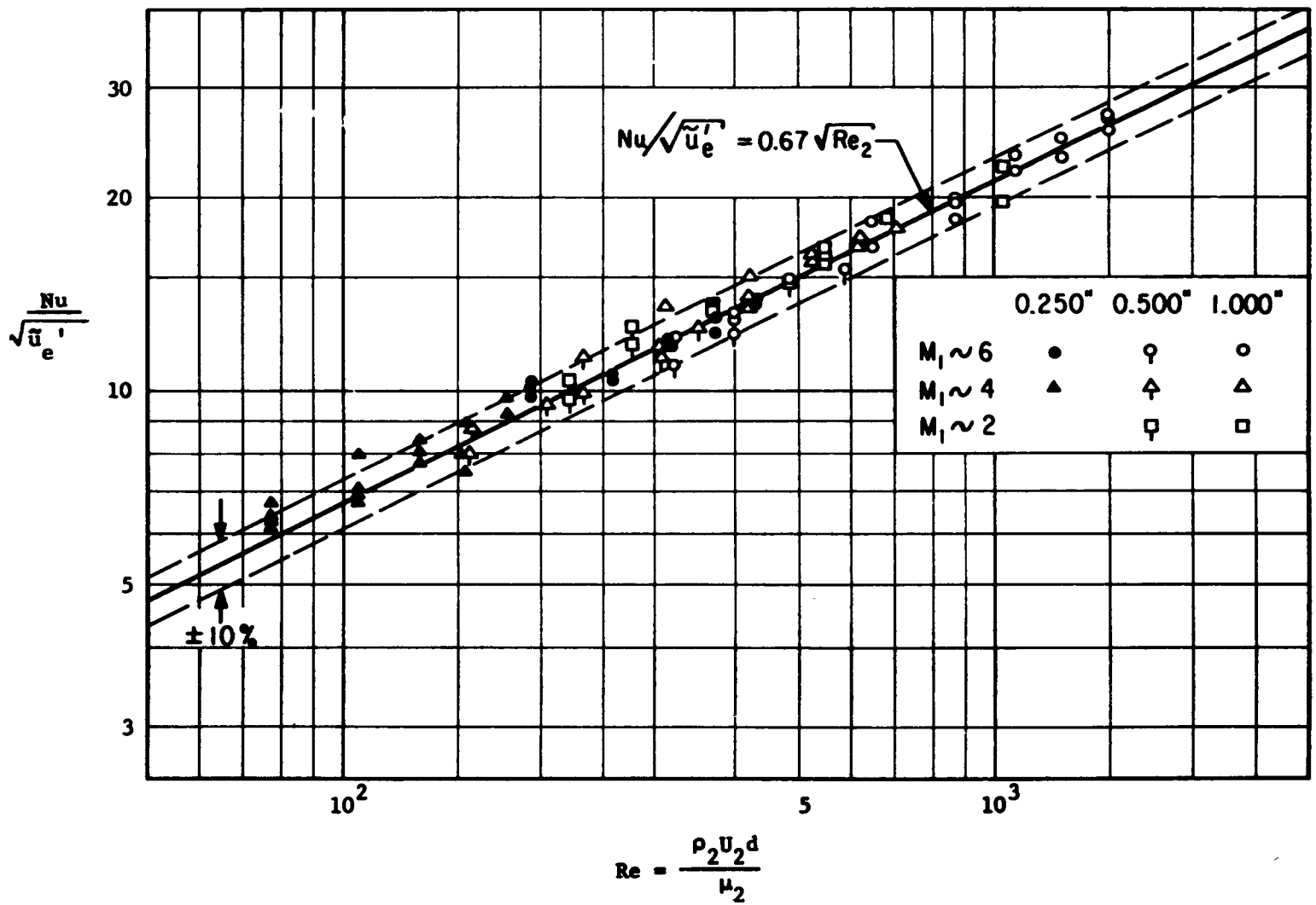

FIGURE 7. COMPARISON OF MEASURED STAGNATION POINT HEAT TRANSFER WITH CONTINUUM BOUNDARY LAYER THEORY

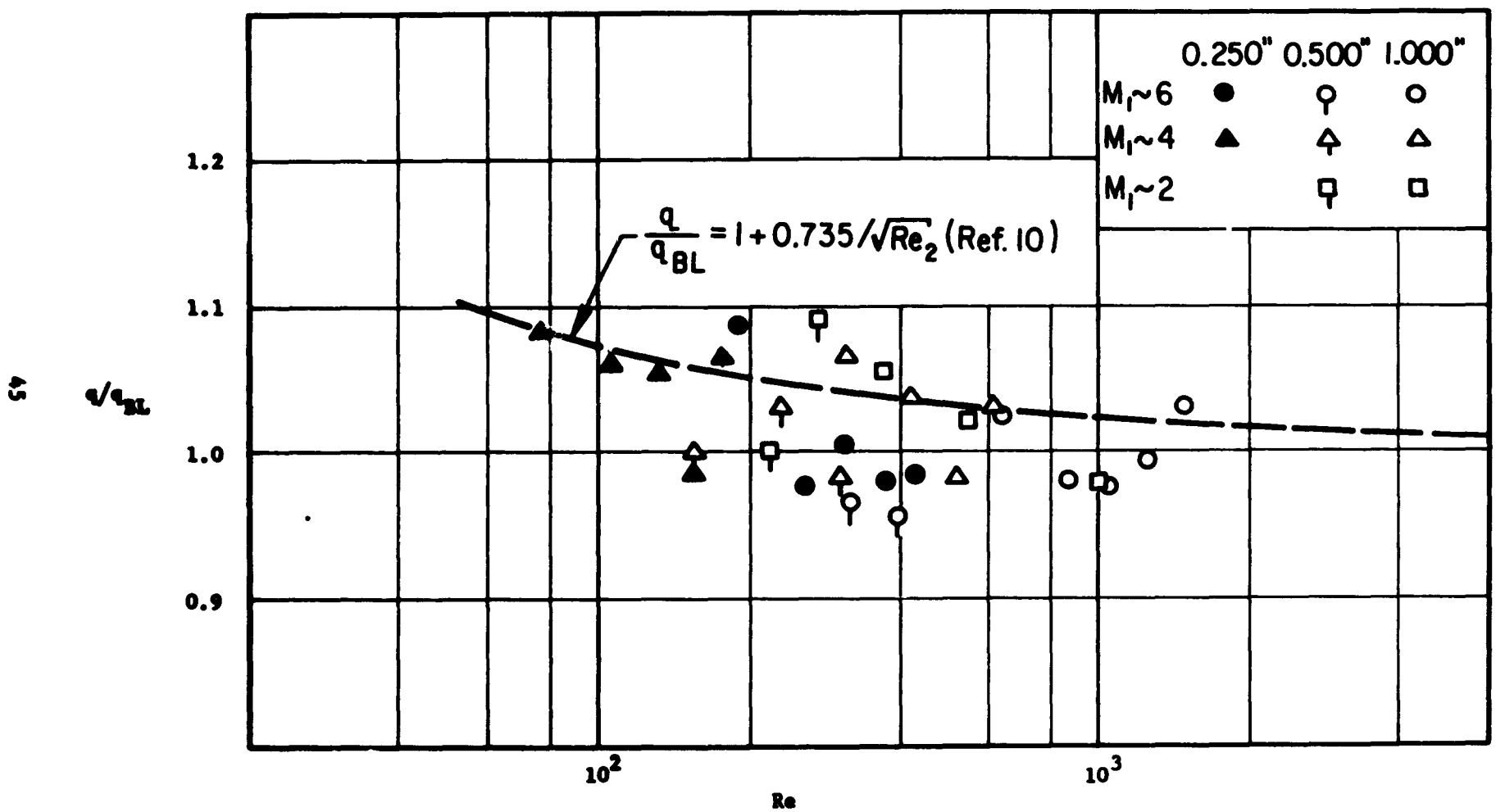

FIGURE 8. RATIO OF AVERAGE VALUES OF MEASURED STAGNATION POINT HEAT TRANSFER TO CONTINUUM BOUNDARY LAYER THEORY

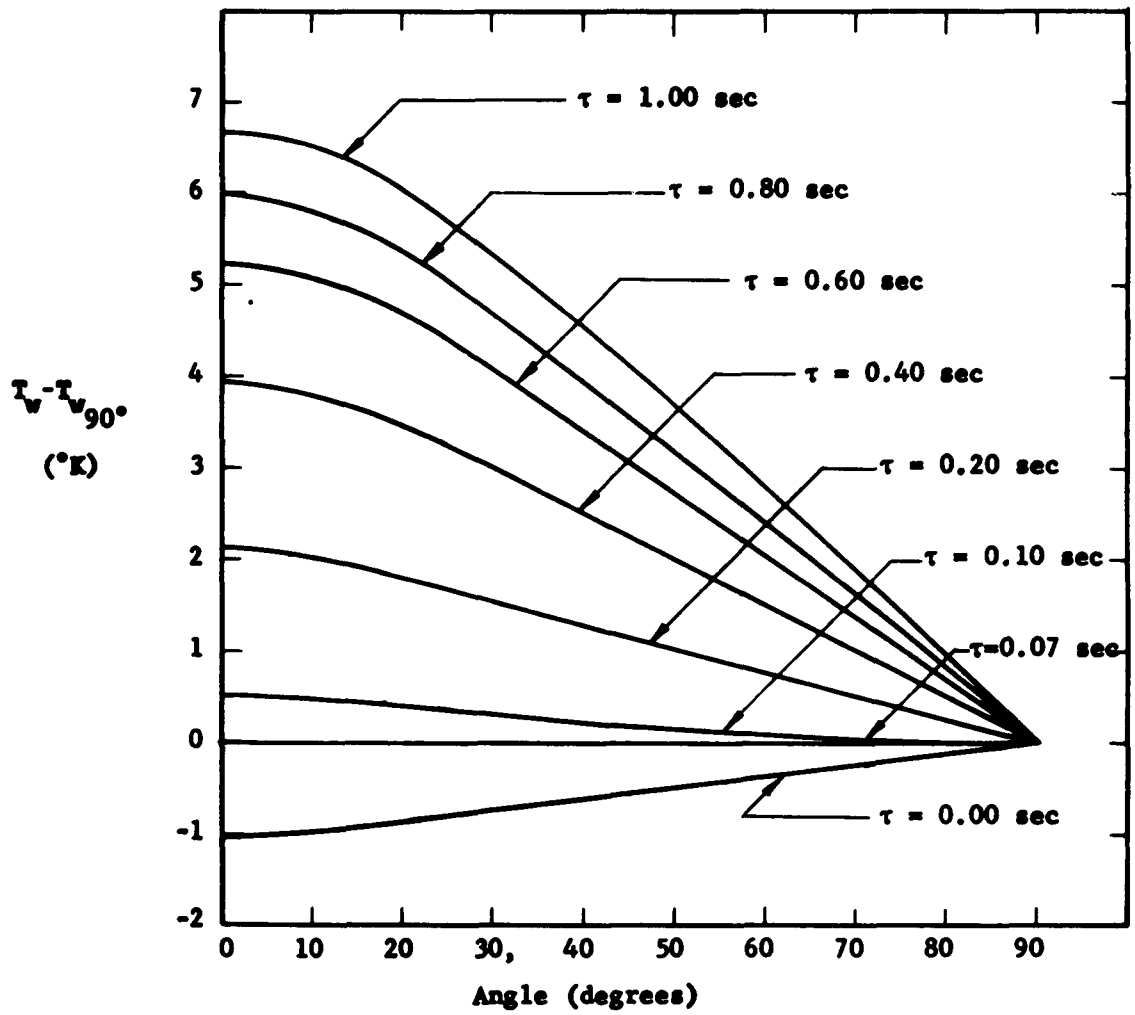

FIGURE 9. TYPICAL WALL TEMPERATURE DISTRIBUTION AT VARIOUS TIMES

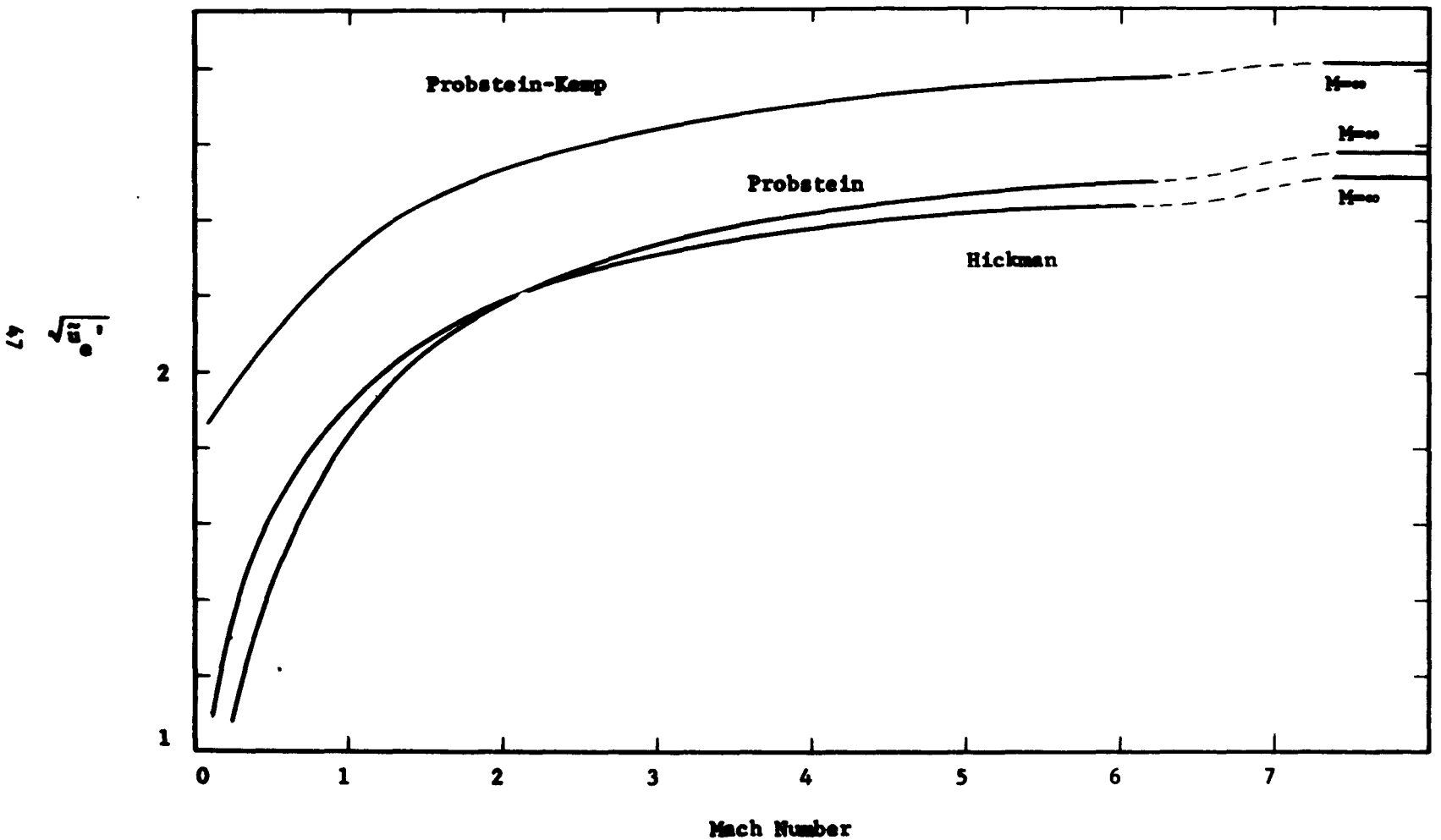

FIGURE 10. COMPARISON OF NON-DIMENSIONAL VELOCITY GRADIENTS AS FUNCTIONS OF MACH NUMBER

Aeronautical Research Laboratories, Wright-Patterson AFB, O. SUPERSONIC STAGNATION POINT HEAT TRANSFER TO HEMISPHERE CYLINDERS AT LOW REYNOLDS NUMBERS by H. Tong, W.H. Giedt, U. of Calif., Berkeley, Calif. February 1963. 47 p. incl. illus. (Project 7064; Task 7064-01) (Contract AF 33(657)-8607) (ARL 63-25) Unclassified Report

Stagnation point heat transfer at low Reynolds numbers in a supersonic air stream was investigated experimentally. A transient technique was employed using precooled thin-walled hemisphere-cylinder models. Tests were conducted at nominal Mach numbers of 2, 4, and 6 and in the Reynolds number range of 80 to 1500. Results are best represented by continuum boundary layer theory. Scatter was about ±10 per cent, so that any possible small shock wave-vorticity effect at the lower values of Reynolds number could not be identified.

(over)

UNCLASSIFIED

UNCLASSIFIED
UNCLASSIFIED
UNCLASSIFIED
UNCLASSIFIED
Aeronautical Research Laboratories, Wright-Patterson AFB, O. SUPERSONIC STAGNATION POINT HEAT TRANSFER TO HEMISPHERE CYLINDERS AT LOW REYNOLDS NUMBERS by H. Tong, W.H. Giedt, U. of Calif., Berkeley, Calif. February 1963. 47 p. incl. illus. (Project 7064; Task 7064-01) (Contract AF 33(657)-8607) (ARL 63-25) Unclassified Report
Stagnation point heat transfer at low Reynolds numbers in a supersonic air stream was investigated experimentally. A transient technique was employed using precooled thin-walled hemisphere-cylinder models. Tests were conducted at nominal Mach numbers of 2, 4, and 6 and in the Reynolds number range of 80 to 1500. Results are best represented by continuum boundary layer theory. Scatter was about ±10 per cent, so that any possible small shock wave-vorticity effect at the lower values of Reynolds number could not be identified.
(over)
UNCLASSIFIED
UNCLASSIFIED
UNCLASSIFIED
UNCLASSIFIED